


Magnon-phonon interaction and the underlying role of the Pauli exclusion principleT. J. Sjöstrand  and F. Aryasetiawan*Department of Physics, Division of Mathematical Physics, Lund University, Professorsgatan 1, 223 62 Lund, Sweden*

(Received 2 November 2021; accepted 12 January 2022; published 26 January 2022; corrected 5 December 2022)

The magnon-phonon interaction is receiving growing attention due to its key role in spin caloritronics and the emerging field of acoustic spintronics. At resonance, this magnetoelastic interaction forms magnon polarons, which underpin exotic phenomena such as magnonic heat currents and phononic spin, but is mostly investigated using mesoscopic spin-lattice models. Motivated to integrate the magnon-phonon interaction into first-principles many-body electronic structure theory, we set out to derive the exchange contribution, which is subtler than the spin-orbit contribution, using Schwinger functional derivatives. To avoid having to solve the famous Hedin–Baym equations self-consistently, the phonons are treated as perturbations to the electronic structure. A formalism based on imposing a crossing-symmetric electron-electron interaction is developed in order to treat charge and spin on equal footing to respect the Pauli exclusion principle. Due to spin conservation, the magnon-phonon interaction first enters to second order through the magnon-magnon interaction, which renormalizes the magnons. We show by iteration that the magnon-magnon interaction contains a “screened T matrix” term and an arguably more important term which, in the local-spin limit, enables first-principles phonon emission and absorption amplitudes, predicted by phenomenological magnetoelastic models. These terms are, respectively, of first and second order in the *screened collective* four-point interaction \mathcal{W} —a crossing-symmetric analog of Hedin’s W . Proof-of-principle results are presented at varying temperatures for an isotropic magnon spectrum in three dimensions in the presence of a flat optical phonon branch.

DOI: [10.1103/PhysRevB.105.014433](https://doi.org/10.1103/PhysRevB.105.014433)**I. INTRODUCTION**

Magnons and phonons are ubiquitous bosonic quasiparticles in condensed-matter physics. Magnons denote collective spin flips—spin fluctuations with spin \hbar and with dispersion and lifetime accessed from the magnetic susceptibility, commonly probed by inelastic neutron scattering. Phonons denote collective lattice deformations, carry no intrinsic spin in the absence of spin-phonon interaction, and are accessed from the charge susceptibility, also commonly probed by inelastic neutron scattering. The two quasiparticles have very distinct physical properties and applications.

Phonons are first and foremost major heat carriers and prevent overheating in microelectronics, although a major issue is that downscaled electronics have a large electron-phonon interaction that inhibits the heat dissipation. The electron-phonon interaction also has positive usages, such as boosting thermoelectric generators to reduce environmental waste [1]. Phonons are employed in cavity optomechanics, with applications ranging from gravitational wave detection to quantum metrology, where phononic crystal cavities are often used to confine sound [2], and laser detuning is used to transfer energy to or from cavity phonons for mechanical amplification or cooling purposes [3]. Magnons, on the other hand, are well

known to dissipate Zeeman energy and relax magnetization but are also used practically for information transport and processing in the emerging field of magnonics, which aims to achieve downscaled and faster computing by pushing for increased magnon speeds, lifetimes, and mean free paths [4,5]. A difficulty in magnon spintronics/electronics is converting information stored in electronic spin/charge to and from the processing magnonic subsystem [6]. Magnons also allow for room-temperature condensation when exposed to microwave pumping [7,8], and through their scattering with electrons, magnons work as a possible pairing glue in unconventional superconductors [9,10]. It follows that a unified picture of superconductivity should necessarily be equipped with proper accounting of both phonons and magnons. The two generally cannot be adiabatically separated, which correlates their dynamics and opens the door to exotic phenomena with novel applications.

The magnon-phonon interaction is strong in manganites [11], nickel nanomagnets and nanopatterned magnetic structures [12,13], yttrium iron garnet [14], polycrystalline BiFeO₃ [15], Eu_{0.75}Y_{0.25}MnO₃ [16], and many other multiferroics and also in ferromagnets such as bcc iron [17,18]. Depending on the relative scattering strength of magnons and phonons in magnetic insulators, the interaction can either increase or decrease the spin Seebeck effect [19–23], a thermoelectric effect that converts temperature gradients to spin currents. This puts the magnon-phonon interaction at the core of spin caloritronics [24], where coupled spin-heat currents are studied—a path to green devices with waste heat recycling capabilities. Another promising direction is acoustic spintronics, initiated

Published by the American Physical Society under the terms of the Creative Commons Attribution 4.0 International license. Further distribution of this work must maintain attribution to the author(s) and the published article’s title, journal citation, and DOI.

by the room-temperature “spintronics battery” in yttrium iron garnet, based on acoustic spin pumping by magnon-phonon resonance [25,26]. The magnon-phonon interaction also leads to a thermal conductivity increase upon magnetic ordering in geometrically frustrated magnets [27], magnonic heat currents [28], and phononic spin [29–31] in quantum magnets and enables photodrive of curved domain walls [32]. It has also provided a mechanism for the thermal Hall effect [33], where local nonequilibrium between magnons and phonons can be achieved optically [34]. We conclude this acclamation of the magnon-phonon interaction by mentioning its link to the coexistence of superconductivity and charge-density waves in high-temperature superconducting copper oxides [35] and to condensation of hybrid magnetoelastic bosons [36].

Prior to such exciting developments, the magnon-phonon interaction was mainly theoretically investigated using spin-lattice models, owing to the success of the Landau-Lifshitz-Gilbert approach to describe mesoscopic magnetization dynamics [37], where precession and damping are included but faster superposed effects are neglected. The initial field-theoretic works in this direction by Abrahams and Kittel were focused on ferromagnets [38–40] and based on tuning a macroscopic magnon-phonon interaction obtained from a postulated magnetoelastic free-energy density to match observed magnetostriction and tuning a pseudodipolar spin-spin interaction to match observed anisotropy. The famous phonon emission and absorption terms were identified as leading terms. Since then, many spin-lattice model studies have contributed to further insights into the interaction in ferro-, ferri-, antiferro- and metamagnets, as well as in complicated setups in and out of equilibrium [21,41–63]. Self-consistent theories of coupled magnetoelastic modes induced by a spatially varying temperature [64] and of phonon pumping based on magnon-number-conserving processes [65] are two interesting recent developments, but these and the above examples contain parameters whose connection to the elementary electronic structure is not fully understood.

The first step towards a first-principles spin-lattice dynamics was arguably taken within time-dependent density functional theory [66], in which molecular dynamics was studied in conjunction with an adiabatically separated spin-density matrix, albeit with a limited treatment of dissipation and temperature. Another major step was the extension of the Landau-Lifshitz-Gilbert approach to account for short-time nutation of the magnetization [67], caused by the moment of inertia and requiring microscopic treatments to access a retarded exchange interaction [68]. A third noteworthy step was based on an action formalism, which provided a minimal bilinear model in which spin and lattice variables were treated on equal footing [69]. What is yet needed is a field-theoretic treatment of the exchange-mediated magnon-phonon interaction, which necessitates a foundation in the electronic structure where the simultaneous screening of charge and spin is physically guided by the Pauli exclusion principle.

This work therefore aims to derive, from the underlying electronic structure, the magnon renormalization due to the exchange-mediated magnon-phonon interaction, which is known to be important at short wavelengths [63]. We leave out the less subtle anisotropy contribution due to the spin-

orbit interaction, and the thermal equilibrium that we will assume can readily be extended to nonequilibrium, although the general ideas will still apply. Since we focus on magnons, we treat phonons as perturbations to avoid having to self-consistently solve the Hedin-Baym equations [70] for coupled electron and phonon systems. Phonons can thus be accounted for at the end of the derivation by a method of replacements [71]. A crossing-symmetric formalism based on Hedin’s is presented in which charge and spin are treated on equal footing. Without spin-orbit interaction, spin conservation forbids magnon-phonon conversion but allows for magnon-number-conserving magnon-phonon interaction [63], which enters to second order in the magnon-magnon interaction and thus renormalizes the magnons. We call this contribution the phonon-assisted magnon-magnon (PAMM) interaction throughout this work.

We will go through the approximations needed to arrive at an expression for the PAMM interaction of the same form as that obtained from phenomenological magnetoelastic models, like in Ref. [63], but with first-principles access to the parameters. The most crucial step is the two-point approximation, which reduces the so-called spin-flip interaction (which contains the magnon-magnon interaction and thus also the PAMM interaction) from a four-point to a two-point quantity. By applying the theory to a simple model, we show how the PAMM interaction leads to not only dissipative broadening of the magnon spectrum but also Hubbard-like splittings. In an upcoming publication, a semirelativistic extension will be presented in which the orbital magnetic moment and the spin-orbit interaction will be included in addition to the exchange contribution considered here.

This paper is organized as follows: in Sec. II we present the formal theory based on Schwinger functional derivatives, in which crossing symmetry is used to put charge and spin on equal footing. In Sec. III a series of approximations is made, which allows for a simple expression of the PAMM interaction. In Sec. IV, a minimal model is considered in which the effect of phonons on the magnon spectrum is considered. Finally, in Sec. V we summarize the work and give an outlook on future developments.

II. FORMAL THEORY

A. Setting the scene

The main goal of this work is to derive the effects of the magnon-phonon interaction on the magnon spectra from first principles in the absence of spin-orbit interaction or other relativistic effects. As explained in the Introduction, this is done by finding an explicit expression for the PAMM interaction, which yields the leading-order magnon renormalization due to phonons. We assume that the orbital angular momentum is quenched in the solid and therefore assume that the magnons are exclusively attributed to the spin fluctuations. The nonrelativistic contribution to the magnon-phonon interaction originates from the exchange interaction and is obtained self-consistently from the Hedin-Baym equations for systems in which both the electrons and the lattice fluctuate [70]. Unfortunately, this self-consistency not only makes practical calculations costly but also clouds the connection to spin-lattice models.

However, it is well known that due to the high-energy (plasmonic) charge screening of the electronic subsystem it is crucial to calculate the phonon Green's function D after an initial electronic structure calculation. Having obtained phonons in such a simplified electronic surrounding, it is natural to compute the electronic structure in the presence of these approximate phonons. This can easily be done in Hedin's formalism by correcting the well-known screened electron-electron interaction W by an additional term WDW containing an intermediate phonon [71]. Since the effects of the approximate phonons exclusively enter through this quantity, it is possible to first derive the spin-fluctuation spectrum as a functional of W , i.e., in a rigid lattice, and then replace the latter by $W + WDW$ to account for the magnon-phonon interaction. We can thus forget about the lattice dynamics completely for now—its consequence is easily corrected for at the end. In principle, it is possible to compute how the resulting magnons affect the electronic structure and “next-iteration phonons,” but this work focuses on the effect of phonons on magnons.

B. A crossing-symmetric starting point

Since equilibrium magnons and phonons are excited thermally, it is natural to work with a finite-temperature formalism, in which an appropriate starting point is the grand canonical Hamiltonian, defined as $\hat{K} = \hat{H} - \mu\hat{N}$, where \hat{H} is the Hamiltonian of the electronic system, μ is the chemical potential, and \hat{N} is the number operator. In an orthonormal Wannier basis, this takes the form

$$\hat{K} = [h(\mathbf{12}) - \delta_{\mathbf{12}}\mu]\hat{c}_{\sigma_1}^\dagger(\mathbf{1})\hat{c}_{\sigma_1}(\mathbf{2}) + \frac{1}{2}v(\mathbf{12},\mathbf{34})\hat{c}_{\sigma_1}^\dagger(\mathbf{1})\hat{c}_{\sigma_4}^\dagger(\mathbf{4})\hat{c}_{\sigma_4}(\mathbf{3})\hat{c}_{\sigma_1}(\mathbf{2}), \quad (1)$$

where h is the hopping matrix and

$$v(\mathbf{12},\mathbf{34}) = \int d\mathbf{x}d\mathbf{y} \frac{w_{n_1\mathbf{R}_1}^*(\mathbf{x})w_{n_2\mathbf{R}_2}(\mathbf{x})w_{n_3\mathbf{R}_3}(\mathbf{y})w_{n_4\mathbf{R}_4}^*(\mathbf{y})}{|\mathbf{x} - \mathbf{y}|} \quad (2)$$

are the Coulomb integrals in the Wannier basis $\{w_{n_i\mathbf{R}_i}\}$, which fulfill the inversion symmetry $v(\mathbf{12},\mathbf{34}) = v(\mathbf{43},\mathbf{21})$. The Wannier functions are assumed to be spin independent for simplicity. In Eq. (1) and the following, we use Einstein's summation convention and Hartree's atomic units, where $\hbar = m_e = e = a_0 = 1$, and let the electron charge be +1 rather than -1 for convenience. The spin index $\sigma_i = \uparrow, \downarrow$ is kept explicit, whereas the Wannier orbital n_i and unit cell \mathbf{T}_i are condensed into index i . To describe the interplay between charge and spin it is key to start from a crossing-symmetric interaction which encodes the Pauli exclusion principle in its definition. This utilizes the fact that the local part of a spin-conserving interaction between a \downarrow and \uparrow electron can be reinterpreted as a simultaneous spin flip of the two, with both processes conserving the total spin locally.

Using anticommutation, it is possible to reformulate the interaction term in Eq. (1), which we call \hat{K}_{int} , into a crossing-symmetric form. The result is

$$\hat{K}_{\text{int}} = \frac{1}{2}v_{\sigma_3\sigma_4}^{\sigma_1\sigma_2}(\mathbf{12},\mathbf{34})\hat{c}_{\sigma_1}^\dagger(\mathbf{1})\hat{c}_{\sigma_4}^\dagger(\mathbf{4})\hat{c}_{\sigma_3}(\mathbf{3})\hat{c}_{\sigma_2}(\mathbf{2}). \quad (3)$$

The spin-dependent interaction can be written in the Pauli form ($\mu = 0, x, y, z$)

$$v_{\sigma_3\sigma_4}^{\sigma_1\sigma_2}(\mathbf{12},\mathbf{34}) = -v_{\sigma_2\sigma_4}^{\sigma_1\sigma_3}(\mathbf{13},\mathbf{24}) \quad (4)$$

$$= \sigma_{\sigma_1\sigma_2}^{\mu_1} v_{\mu_1\mu_2}(\mathbf{12},\mathbf{34})\sigma_{\sigma_4\sigma_3}^{\mu_2}, \quad (5)$$

where the first equality shows the crossing symmetry and

$$v_{\mu_1\mu_2}(\mathbf{12},\mathbf{34}) = \frac{\delta_{\mu_1\mu_2}}{2} \left[\delta_{\mu_1 0} v(\mathbf{12},\mathbf{34}) - \frac{1}{2} v(\mathbf{13},\mathbf{24}) \right]. \quad (6)$$

This is the origin of the exchange interaction between spins in the Heisenberg model. It forbids unphysical local interactions between two electrons of identical spin in the many-body treatment, which is to follow, and is thus the most appealing form allowed by the Fierz ambiguity [72].

C. Schwinger's functional derivative method

We now use Schwinger functional derivatives, with the goal of obtaining the magnon spectrum from the electronic structure. The starting point is the imaginary-time Green's function for an electron in the Dirac picture

$$\mathcal{G}_{\sigma_1\sigma_2}(12) = -\frac{\text{Tr} \left[e^{-\beta\hat{K}} \hat{\mathcal{T}} \hat{S} \hat{c}_{\sigma_1}(1) \hat{c}_{\sigma_2}^\dagger(2) \right]}{\text{Tr} \left(e^{-\beta\hat{K}} \hat{S} \right)}, \quad (7)$$

where the imaginary times τ_i , which are hidden in the combined indices $i = (\mathbf{i}, \tau_i)$, are assumed to be between zero and the “thermodynamic beta,” $\beta = 1/k_B T$. Furthermore, $\hat{\mathcal{T}}$ is the time-ordering operator in imaginary time, $\hat{c}_{\sigma_1}(1) = e^{\hat{K}\tau_1} \hat{c}_{\sigma_1}(\mathbf{1}) e^{-\hat{K}\tau_1}$ is the annihilation operator in the Dirac picture, and \hat{S} is the imaginary-time evolution operator from zero to β due to a virtual (external) two-point field φ^{ext} , i.e.,

$$\hat{S} = \hat{\mathcal{T}} \exp \left[-\varphi_{\sigma_3\sigma_4}^{\text{ext}}(34) \hat{c}_{\sigma_3}^\dagger(3) \hat{c}_{\sigma_4}(4) \right], \quad (8)$$

with implicit integration from zero to β over both τ_3 and τ_4 . The equation of motion for \mathcal{G} can easily be obtained from the Heisenberg equation, which reads

$$-\partial_{\tau_1} \hat{c}_{\sigma_1}(1) = [\hat{c}_{\sigma_1}(1), \hat{K}]. \quad (9)$$

This commutator is evaluated using Eqs. (1) and (3) and results in the equation of motion

$$\begin{aligned} & \delta_{\sigma_1\sigma_2} \delta_{12} \\ &= -\left\{ \delta_{\sigma_1\sigma_3} [\delta_{13} \partial_{\tau_1} + k(13)] + \varphi_{\sigma_1\sigma_3}^{\text{ext}}(13) \right\} \mathcal{G}_{\sigma_3\sigma_2}(32) \\ &+ v_{\sigma_4\sigma_5}^{\sigma_1\sigma_3}(13,45) \frac{\text{Tr} \left[e^{-\beta\hat{K}} \hat{\mathcal{T}} \hat{S} \hat{c}_{\sigma_5}^\dagger(5^+) \hat{c}_{\sigma_4}(4) \hat{c}_{\sigma_3}(3) \hat{c}_{\sigma_2}^\dagger(2) \right]}{\text{Tr} \left(e^{-\beta\hat{K}} \hat{S} \right)}, \end{aligned} \quad (10)$$

where we have defined $[\delta_{\tau_1\tau_2} = \delta(\tau_1 - \tau_2)]$

$$k(13) = \delta_{\tau_1\tau_3} [h(\mathbf{13}) - \delta_{13}\mu], \quad (11)$$

$$v_{\sigma_4\sigma_5}^{\sigma_1\sigma_3}(13,45) = \delta_{\tau_1\tau_3} \delta_{\tau_3\tau_4} \delta_{\tau_4\tau_5} v_{\sigma_4\sigma_5}^{\sigma_1\sigma_3}(\mathbf{13},\mathbf{45}). \quad (12)$$

The last term in Eq. (10) contains the two-electron Green's function, which in terms of \mathcal{G} reads

$$\begin{aligned} & \frac{\text{Tr} \left[e^{-\beta\hat{K}} \hat{\mathcal{T}} \hat{S} \hat{c}_{\sigma_5}^\dagger(5^+) \hat{c}_{\sigma_4}(4) \hat{c}_{\sigma_3}(3) \hat{c}_{\sigma_2}^\dagger(2) \right]}{\text{Tr} \left(e^{-\beta\hat{K}} \hat{S} \right)} \\ &= -\mathcal{G}_{\sigma_3\sigma_2}(32) \mathcal{G}_{\sigma_4\sigma_5}(45^+) + \frac{\delta \mathcal{G}_{\sigma_3\sigma_2}(32)}{\delta \varphi_{\sigma_5\sigma_4}^{\text{ext}}(5^+4)}, \end{aligned} \quad (13)$$

as verified with the chain rule by differentiating Eq. (7), where the φ^{ext} dependence is contained in \hat{S} through Eq. (8). Inserting Eq. (13) into Eq. (10) shows that the term containing $\delta \mathcal{G} / \delta \varphi^{\text{ext}}$ complicates the access to a practically useful

functional of \mathcal{G}^{-1} in terms of \mathcal{G} . In Hedin's formalism [73], which does not impose a crossing-symmetric interaction, the analogous term defines the self-energy Σ . But unlike Hedin's formalism, the $\delta\mathcal{G}/\delta\varphi^{\text{ext}}$ contribution to Eq. (10) does not correspond to exchange and correlation, but to half the Hartree-Fock potential plus correlations. The crossing-symmetric starting point thus hints at a pathology of treating the two terms in Eq. (13) asymmetrically, so we avoid introducing Σ . However, to invert Eq. (10) using the chain rule $\delta\mathcal{G} = -\mathcal{G}\delta\mathcal{G}^{-1}\mathcal{G}$ is unavoidable, so that both terms in Eq. (13) contain a suitable factor of \mathcal{G} , yielding

$$\mathcal{G}_{\sigma_1\sigma_2}^{-1}(I2) = -[\delta_{I2}\partial_{I_1} + k(I2)]\delta_{\sigma_1\sigma_2} - \varphi_{\sigma_1\sigma_2}^{\text{tot}}(I^+2). \quad (14)$$

The total field splits into two components,

$$\varphi_{\sigma_1\sigma_2}^{\text{tot}}(I^+2) = \varphi_{\sigma_1\sigma_2}^{\text{ext}}(I^+2) + \varphi_{\sigma_1\sigma_2}^{\text{ind}}(I^+2), \quad (15)$$

where the induced field reads

$$\begin{aligned} \varphi_{\sigma_1\sigma_2}^{\text{ind}}(I^+2) &= v_{\sigma_3\sigma_4}^{\sigma_1\sigma_2}(I2, 34)\mathcal{G}_{\sigma_3\sigma_4}(34^+) \\ &\quad - v_{\sigma_4\sigma_5}^{\sigma_1\sigma_3}(I3, 45)\mathcal{G}_{\sigma_3\sigma_6}(36^+) \frac{\delta\varphi_{\sigma_6\sigma_2}^{\text{tot}}(6^+2)}{\delta\varphi_{\sigma_5\sigma_4}^{\text{ext}}(5^+4)}. \end{aligned} \quad (16)$$

This is the ‘‘mass operator’’ in Hedin's theory. Since this is varied when deriving the spin susceptibility, the Green's function has to be kept nondiagonal in the spin index until the end, despite the absence of spin-orbit interaction. Before continuing along these lines, we turn to the four-vector representation in Sec. IID, where the connection to the macroscopic Maxwell fields is clarified.

D. Four-vector representation

The external, induced, and total fields can all be written in the generic Pauli form

$$\varphi_{\sigma_1\sigma_2}(I^+2) = \sigma_{\sigma_1\sigma_2}^{\mu} \varphi_{\mu}(I^+2), \quad (17)$$

$$\varphi_{\mu}(I^+2) = \frac{1}{2}\sigma_{\sigma_4\sigma_3}^{\mu} \varphi_{\sigma_3\sigma_4}(I^+2), \quad (18)$$

with four-vector index $\mu = 0, x, y, z$, and

$$\varphi_{\mu}(I^+2) = (\phi(I^+2), -\frac{1}{2}\mathbf{B}_i(I^+2)). \quad (19)$$

Here, ϕ is the electric scalar potential ($E_i = -\partial_i\phi$), B_i is the magnetic flux density, and $\frac{1}{2}$ is the Bohr magneton. To be consistent with Eqs. (17) and (18), field derivatives must be related as

$$\frac{\delta}{\delta\varphi_{\sigma_1\sigma_2}(I^+2)} = \frac{1}{2}\sigma_{\sigma_2\sigma_1}^{\mu} \frac{\delta}{\varphi_{\mu}(I^+2)}, \quad (20)$$

$$\frac{\delta}{\delta\varphi_{\mu}(I^+2)} = \sigma_{\sigma_3\sigma_4}^{\mu} \frac{\delta}{\delta\varphi_{\sigma_3\sigma_4}(I^+2)}. \quad (21)$$

The spin-density matrix ϱ , which is related to the Green's function through the simple relation

$$\varrho_{\sigma_1\sigma_2}(I^+2) = \mathcal{G}_{\sigma_2\sigma_1}(2I^+), \quad (22)$$

has the same Pauli form as the field derivatives, namely,

$$\varrho_{\sigma_1\sigma_2}(I^+2) = \frac{1}{2}\sigma_{\sigma_1\sigma_2}^{\mu} \varrho_{\mu}(I^+2), \quad (23)$$

$$\varrho_{\mu}(I^+2) = \sigma_{\sigma_3\sigma_4}^{\mu} \varrho_{\sigma_3\sigma_4}(I^+2), \quad (24)$$

where, notably, $\varrho_0 = n$ is the electronic density and $\varrho_z = m$ is the spin magnetization. Likewise, the spin-density derivatives are in the same form as the fields,

$$\frac{\delta}{\delta\varrho_{\sigma_1\sigma_2}(I^+2)} = \sigma_{\sigma_1\sigma_2}^{\mu} \frac{\delta}{\varrho_{\mu}(I^+2)}, \quad (25)$$

$$\frac{\delta}{\delta\varrho_{\mu}(I^+2)} = \frac{1}{2}\sigma_{\sigma_4\sigma_3}^{\mu} \frac{\delta}{\delta\varrho_{\sigma_3\sigma_4}(I^+2)}. \quad (26)$$

The four-vector representation of Eq. (16) is obtained from Eqs. (5), (12), (18), (21), (22), and (23), yielding

$$\begin{aligned} \varphi_{\mu_1}^{\text{ind}}(I^+2) &= v_{\mu_1\mu_3}(I2, 34)\varrho_{\mu_3}(4^+3) \\ &\quad - \frac{1}{4}\text{tr}(\sigma^{\mu_1}\sigma^{\mu_2}\sigma^{\mu_3}\sigma^{\mu_4})v_{\mu_2\mu_5}(I3, 45)\varrho_{\mu_3}(6^+3) \frac{\delta\varphi_{\mu_4}^{\text{tot}}(6^+2)}{\delta\varphi_{\mu_5}^{\text{ext}}(5^+4)}, \end{aligned} \quad (27)$$

where $\text{tr}(\sigma^{\mu_1}\sigma^{\mu_2}) = 2\delta_{\mu_1\mu_2}$ is used twice in the first term. The trace in the second term can be evaluated but contains many terms. This shows the benefit of the usual ‘‘spin representation’’; another benefit is that it naturally expresses the crossing symmetry, like in Eq. (4). Since this will be relevant later when deriving the spin-flip interaction, we will return to the spin representation, but we first stress the correspondence to field quantities in the macroscopic Maxwell theory, reading [74]

$$\varphi_{\mu}^{\text{tot}} = (\phi, -\frac{1}{2}\mathbf{B}_i), \quad (28)$$

$$\varphi_{\mu}^{\text{ext}} = (\frac{1}{\varepsilon_0}\phi_D, -\frac{1}{2}\mu_0\mathbf{H}_i), \quad (29)$$

$$\varphi_{\mu}^{\text{ind}} = (-\frac{1}{\varepsilon_0}\phi_P, -\frac{1}{2}\mu_0\mathbf{M}_i), \quad (30)$$

where ϕ_D and ϕ_P are scalar potentials for the electric displacement and polarization fields, which are assumed to be conservative, i.e., $D_i = -\partial_i\phi_D$ and $P_i = -\partial_i\phi_P$. In addition, H_i is the inductive magnetic field, and M_i is the magnetization field. For clarity, we have refrained from utilizing $\varepsilon_0 = 1/4\pi$ and $\mu_0 = 4\pi\alpha^2$ in atomic units, where $\alpha \approx 1/137$ is the fine-structure constant. With this correspondence, it is easy to identify the inverse relative dielectric function as well as relative permeability as

$$\varepsilon_r^{-1}(I2, 34) = \frac{\delta\varphi_0^{\text{tot}}(1^+2)}{\delta\varphi_0^{\text{ext}}(3^+4)}, \quad (31)$$

$$\mu_{r_{ij}}(I2, 34) = \frac{\delta\varphi_i^{\text{tot}}(I^+2)}{\delta\varphi_j^{\text{ext}}(3^+4)}. \quad (32)$$

There are also the components $\delta\varphi_0^{\text{tot}}/\delta\varphi_j^{\text{ext}}$ and $\delta\varphi_i^{\text{tot}}/\delta\varphi_0^{\text{ext}}$, which are important in the presence of spin-orbit interaction. Common to all components is the fact that they describe an ‘‘inverse electromagnetic screening factor’’ \mathcal{S} . We therefore define

$$\mathcal{S}_{\mu_1\mu_3}^{-1}(I2, 34) = \frac{\delta\varphi_{\mu_1}^{\text{tot}}(I^+2)}{\delta\varphi_{\mu_3}^{\text{ext}}(3^+4)}. \quad (33)$$

The static limits of the charge-charge and spin-spin components are small in metals and diamagnets, respectively, whereas in ferromagnets the latter instead diverges. The required higher-order field variations in ferromagnets are implicitly included in the formalism despite the fact that only the linear screening \mathcal{S} appears explicitly.

E. Screened collective four-point interaction

Having established connections to Maxwell's theory, we continue on the path towards the PAMM interaction. In Eq. (16), the main quantity to find is

$$\mathcal{S}^{-1}|_{\sigma_3\sigma_4}^{\sigma_1\sigma_2}(12, 34) = \frac{\delta\varphi_{\sigma_1\sigma_2}^{\text{tot}}(I+2)}{\delta\varphi_{\sigma_3\sigma_4}^{\text{ext}}(3+4)}. \quad (34)$$

Using Eq. (15) and the chain rule yields

$$\begin{aligned} \mathcal{S}^{-1}|_{\sigma_3\sigma_4}^{\sigma_1\sigma_2}(12, 34) \\ = \delta_{\sigma_1\sigma_3} \delta_{\sigma_2\sigma_4} \delta_{13} \delta_{24} + \mathcal{V}_{\sigma_5\sigma_6}^{\sigma_1\sigma_2}(12, 56) \mathcal{P}_{\sigma_7\sigma_8}^{\sigma_5\sigma_6}(56, 78) \mathcal{S}^{-1}|_{\sigma_3\sigma_4}^{\sigma_7\sigma_8}(78, 34), \end{aligned} \quad (35)$$

where

$$\mathcal{V}_{\sigma_3\sigma_4}^{\sigma_1\sigma_2}(12, 34) = \frac{\delta\varphi_{\sigma_1\sigma_2}^{\text{ind}}(I+2)}{\delta\varrho_{\sigma_4\sigma_3}(4+3)} \quad (36)$$

is the *collective* four-point interaction, which in Hedin's formalism amounts to the sum of Coulomb interaction and irreducible four-point vertex $\delta\Sigma/\delta\mathcal{G}$ [75,76], and

$$\mathcal{P}_{\sigma_3\sigma_4}^{\sigma_1\sigma_2}(12, 34) = \frac{\delta\varrho_{\sigma_2\sigma_1}(2+1)}{\delta\varphi_{\sigma_3\sigma_4}^{\text{tot}}(3+4)} \quad (37)$$

$$= \mathcal{G}_{\sigma_1\sigma_3}(13^+) \mathcal{G}_{\sigma_4\sigma_2}(42^+) \quad (38)$$

is the *free* electron-hole pair propagator, which might also be called the four-point electromagnetic polarization function. By defining the *screened collective* four-point interaction

$$\mathcal{W}_{\sigma_3\sigma_4}^{\sigma_1\sigma_2}(12, 34) = \mathcal{S}^{-1}|_{\sigma_5\sigma_6}^{\sigma_1\sigma_2}(12, 56) \mathcal{V}_{\sigma_3\sigma_4}^{\sigma_5\sigma_6}(56, 34), \quad (39)$$

it is possible to write

$$\begin{aligned} \mathcal{S}^{-1}|_{\sigma_3\sigma_4}^{\sigma_1\sigma_2}(12, 34) = \delta_{\sigma_1\sigma_3} \delta_{\sigma_2\sigma_4} \delta_{13} \delta_{24} \\ + \mathcal{W}_{\sigma_5\sigma_6}^{\sigma_1\sigma_2}(12, 56) \mathcal{P}_{\sigma_3\sigma_4}^{\sigma_5\sigma_6}(56, 34), \end{aligned} \quad (40)$$

which when plugged into Eq. (16) yields

$$\begin{aligned} \varphi_{\sigma_1\sigma_2}^{\text{ind}}(I+2) = 2v_{\sigma_3\sigma_4}^{\sigma_1\sigma_2}(12, 34) \mathcal{G}_{\sigma_3\sigma_4}(34^+) \\ - v_{\sigma_4\sigma_5}^{\sigma_1\sigma_3}(13, 45) \mathcal{G}_{\sigma_3\sigma_6}(36^+) \\ \times \mathcal{G}_{\sigma_7\sigma_5}(75^+) \mathcal{G}_{\sigma_4\sigma_8}(48^+) \mathcal{W}_{\sigma_7\sigma_8}^{\sigma_6\sigma_2}(62, 78). \end{aligned} \quad (41)$$

The first term is the Hartree-Fock potential, where the factor of 2 is a consequence of the crossing symmetry of v in Eq. (4). The second term employs Eq. (38) and contains all correlations through \mathcal{W} , which, like v , fulfils the crossing symmetry

$$\mathcal{W}_{\sigma_3\sigma_4}^{\sigma_1\sigma_2}(12, 34) = -\mathcal{W}_{\sigma_2\sigma_4}^{\sigma_1\sigma_3}(13, 24) \quad (42)$$

or a similar equation if $1\sigma_1$ and $4\sigma_4$ are interchanged. This guarantees that the wave function is antisymmetric when interchanging electrons and is proven by repeating the derivation when initially anticommuting the annihilation operators

in Eq. (3). \mathcal{W} has another symmetry related to pair hopping, proven by using anomalous probing fields which interchange electrons and positrons, but it is of little interest in this work.

F. Spin susceptibility and spin-flip interaction

The *interacting* electron-hole propagator is defined as

$$\mathcal{R}_{\sigma_3\sigma_4}^{\sigma_1\sigma_2}(12, 34) = \frac{\delta\varrho_{\sigma_2\sigma_1}(2+1)}{\delta\varphi_{\sigma_3\sigma_4}^{\text{ext}}(3+4)}, \quad (43)$$

which is analogous to \mathcal{P} in Eq. (37), but with φ^{tot} replaced by φ^{ext} . The physical charge and spin susceptibilities are obtained by contraction, through

$$\mathcal{R}_{\sigma_3\sigma_4}^{\sigma_1\sigma_2}(13) = \mathcal{R}_{\sigma_3\sigma_4}^{\sigma_1\sigma_2}(11, 33), \quad (44)$$

which, with Eqs. (20), (22), and (23), can be expressed as

$$\mathcal{R}_{\sigma_3\sigma_4}^{\sigma_1\sigma_2}(13) = \frac{\sigma_{\sigma_1\sigma_2}^\mu}{2} \frac{\delta\varrho_\mu(I+1)}{\delta\varphi_{\sigma_3\sigma_4}^{\text{ext}}(3+3)} \frac{\sigma_{\sigma_4\sigma_3}^\nu}{2}. \quad (45)$$

Since z is the spin direction, Eq. (45) shows that the transverse spin fluctuations are contained in $\mathcal{R}_{\downarrow\downarrow}^{\uparrow\uparrow}$ and $\mathcal{R}_{\uparrow\uparrow}^{\downarrow\downarrow}$, which yield the magnon spectra through their imaginary parts. Since the two are related by reflection symmetry, we will consider only the former. From (43) and the chain rule, we get

$$\begin{aligned} \mathcal{R}_{\downarrow\downarrow}^{\uparrow\uparrow}(12, 34) = \mathcal{P}_{\downarrow\downarrow}^{\uparrow\uparrow}(12, 34) \\ + \mathcal{P}_{\downarrow\downarrow}^{\uparrow\uparrow}(12, 56) \mathcal{V}_{\downarrow\downarrow}^{\uparrow\uparrow}(56, 78) \mathcal{R}_{\downarrow\downarrow}^{\uparrow\uparrow}(78, 34). \end{aligned} \quad (46)$$

With spin-orbit interaction, this equation would, due to a spin-nondiagonal \mathcal{G} , also couple charge and spin components of \mathcal{R} and, when accounting for phonons, would contain the process of magnon-phonon interconversion [54,63]. This could be solved at the level of the random-phase approximation, but as emphasized earlier, this work focuses on the nonrelativistic magnon-number-conserving processes. The goal is to derive a contribution to the *spin-flip* interaction $\mathcal{V}_{\downarrow\downarrow}^{\uparrow\uparrow}$ describing the simultaneous propagation of spin and charge excitations, which allow for spin conservation and, after the inclusion of phonons, will be shown to contain the PAMM interaction. Since the spin-flip interaction is a four-point quantity, it is necessary to solve for the full four-point $\mathcal{R}_{\downarrow\downarrow}^{\uparrow\uparrow}$ and contract it afterwards according to Eq. (44) to access the spin susceptibility.

III. APPROXIMATE THEORY

A. Low-energy model

The long-range interaction v , which enters the spin-flip interaction through Eqs. (36) and (41), makes calculations very expensive. Trading rigor for clarity, we assume that a renormalized low-energy model has properly been constructed in advance and make the replacement

$$v_{\sigma_3\sigma_4}^{\sigma_1\sigma_2}(12, 34) := \mathcal{U}_{\sigma_3\sigma_4}^{\sigma_1\sigma_2}(I) \delta_{12} \delta_{23} \delta_{34}, \quad (47)$$

$$\mathcal{U}_{\sigma_3\sigma_4}^{\sigma_1\sigma_2}(I) = \frac{\mathcal{U}_{n1}}{2} (\delta_{\sigma_1\sigma_2} \delta_{\sigma_3\sigma_4} - \delta_{\sigma_1\sigma_3} \delta_{\sigma_2\sigma_4}), \quad (48)$$

which assumes an instantaneous, local, and orbital-diagonal interaction, which still fulfils crossing symmetry. This neglects retardation and couplings between different unit cells

and between different orbitals in the same unit cell and is justified if the low-energy electronic structure has a single isolated spin-resolved band at the Fermi energy. This step is easily avoided if needed but is instructive for investigating the magnon-phonon interaction, owing to the fact that a single magnon branch requires only a one-band model.

Since the spin-flip interaction is obtained by varying $\varphi_{\uparrow\downarrow}^{\text{ind}}$, we insert the replacement of Eq. (47) into Eq. (41) and get

$$\begin{aligned} \varphi_{\uparrow\downarrow}^{\text{ind}}(I^+2) &= 2\delta_{I2}\mathcal{U}_{\uparrow\downarrow}^{\uparrow\downarrow}(I)\mathcal{G}_{\uparrow\downarrow}(22^+) \\ &\quad - \mathcal{U}_{\sigma_4\sigma_5}^{\downarrow\sigma_3}(I)\mathcal{G}_{\sigma_3\sigma_6}(16^+) \\ &\quad \times \mathcal{G}_{\sigma_7\sigma_5}(71^+)\mathcal{G}_{\sigma_4\sigma_8}(18^+)\mathcal{W}_{\sigma_7\sigma_8}^{\sigma_6\uparrow}(62, 78), \end{aligned} \quad (49)$$

which, when used in Eq. (36), yields

$$\begin{aligned} \mathcal{V}_{\uparrow\downarrow}^{\uparrow\downarrow}(12, 34) &= 2\delta_{I2}\delta_{23}\delta_{34}\mathcal{U}_{\uparrow\downarrow}^{\uparrow\downarrow}(I) \\ &\quad - 2\delta_{I3}\mathcal{U}_{\uparrow\uparrow}^{\uparrow\uparrow}(I)\mathcal{G}_{\uparrow}(15^+)\mathcal{G}_{\uparrow}(61^+)\mathcal{W}_{\uparrow\uparrow}^{\uparrow\uparrow}(42, 65) \\ &\quad + 2\delta_{I4}\mathcal{U}_{\uparrow\downarrow}^{\uparrow\downarrow}(I)\mathcal{G}_{\downarrow}(15^+)\mathcal{G}_{\uparrow}(16^+)\mathcal{W}_{\uparrow\downarrow}^{\uparrow\downarrow}(52, 36) \\ &\quad - 2\mathcal{U}_{\uparrow\uparrow}^{\uparrow\uparrow}(I)\mathcal{G}_{\downarrow}(16^+)\mathcal{G}_{\uparrow}(71^+)\mathcal{G}_{\uparrow}(18^+) \\ &\quad \times \frac{\delta\mathcal{W}_{\uparrow\uparrow}^{\uparrow\uparrow}(62, 78)}{\delta\mathcal{G}_{\uparrow\uparrow}(34^+)}, \end{aligned} \quad (50)$$

where the crossing symmetries of \mathcal{U} and \mathcal{W} have been used along with the spin diagonality of \mathcal{G} , which is valid in the absence of spin-orbit interaction. \mathcal{U} has been treated as \mathcal{G} independent, in analogy to v in the full Hilbert space. The functional derivative $\delta\mathcal{W}/\delta\mathcal{G}$ will be shown to contain the interaction between spin and charge fluctuations and, when generalized to dynamical lattices, to generate the PAMM interaction. The generalization of Eq. (50) for arbitrary spin components of \mathcal{V} together with Eq. (39) for \mathcal{W} forms a self-consistent set, even when \mathcal{G} and \mathcal{P} are treated as predetermined inputs, for example, from density functional theory. Since this is beyond the reach of present-day computational capacities, we will solve Eq. (50) iteratively.

B. Iterative spin-flip interaction

A practical scheme is iterative rather than self-consistent. The first iteration is obtained by dropping \mathcal{W} on the right-hand side of Eq. (50). Using Eq. (48), the first iteration yields

$$\mathcal{V}_{\uparrow\downarrow}^{\cdot\uparrow\downarrow}(12, 34) = \delta_{I2}\delta_{34}\mathcal{V}_{\uparrow\downarrow}^{\cdot\uparrow\downarrow}(13) = -\delta_{I2}\delta_{23}\delta_{34}\mathcal{U}_{nI}, \quad (51)$$

where the number of \cdot symbols denotes the iteration number. The one-point structure, which also holds for the other spin components of \mathcal{V} , implies that \mathcal{W} has the same two-point structure for all spin components. Since this clearly breaks the crossing symmetry of \mathcal{W} , we use a trick where $\mathcal{W}_c = \mathcal{W} - \mathcal{V} = \mathcal{W}\mathcal{P}\mathcal{V}$ is approximated as

$$\mathcal{W}_{c\sigma_3\sigma_4}^{\sigma_1\sigma_2}(12, 34) \approx \delta_{I2}\delta_{34}\mathcal{W}_{c\sigma_3\sigma_4}^{\sigma_1\sigma_2}(13) - \delta_{I3}\delta_{24}\mathcal{W}_{c\sigma_2\sigma_4}^{\sigma_1\sigma_3}(12), \quad (52)$$

where we, for convenience, denote the two-point interactions as \mathcal{W}_c , although their physical dimensions differ from the four-point interactions by two factors of time. Equation (52) corresponds to keeping direct and exchange matrix elements,

but we have used the crossing symmetry on the latter. Notice that the double counting of the component $\mathcal{W}_c^{\sigma_1\sigma_2}(11)$ introduces no error, unless the imaginary time is discretized. Since our goal is to express the next iteration interaction \mathcal{V}^{\cdot} in terms of \mathcal{G} , \mathcal{V} , and \mathcal{W}_c , it is clear from Eqs. (50), (51), and (52) that it only remains to find expressions for the factors $\delta\mathcal{W}/\delta\mathcal{G}$, with \mathcal{W} corresponding to the two-point reductions in Eq. (52). For arbitrary spin components, it follows from Eqs. (39) and (40) that $\mathcal{W}^{-1} = \mathcal{V}^{-1} - \mathcal{P}$, and consequently, from the chain rule

$$\frac{\delta\mathcal{W}_{\sigma_3\sigma_4}^{\sigma_1\sigma_2}(13)}{\delta\mathcal{G}_{\sigma_5\sigma_6}(56^+)} = \mathcal{W}_{\sigma_7\sigma_8}^{\sigma_1\sigma_2}(17) \frac{\delta\mathcal{P}_{\sigma_9\sigma_{10}}^{\sigma_7\sigma_8}(79)}{\delta\mathcal{G}_{\sigma_5\sigma_6}(56^+)} \mathcal{W}_{\sigma_3\sigma_4}^{\sigma_9\sigma_{10}}(93), \quad (53)$$

where the \mathcal{G} independence of \mathcal{V} in Eq. (51) has been used. The two factors of \mathcal{W} on the right-hand side do, in general, have three-point contributions, but these must vanish due to Eq. (52). From Eq. (38) it follows that

$$\begin{aligned} \frac{\delta\mathcal{P}_{\sigma_9\sigma_{10}}^{\sigma_7\sigma_8}(79)}{\delta\mathcal{G}_{\sigma_5\sigma_6}(56^+)} &= \delta_{\sigma_7\sigma_5}\delta_{\sigma_9\sigma_6}\delta_{75}\delta_{96}\mathcal{G}_{\sigma_{10}\sigma_8}(97^+) \\ &\quad + \delta_{\sigma_{10}\sigma_5}\delta_{\sigma_8\sigma_6}\delta_{95}\delta_{76}\mathcal{G}_{\sigma_7\sigma_9}(79^+). \end{aligned} \quad (54)$$

Using Eqs. (38), (47), (48), (51), (52), (53), and (54), the second iteration of the spin-flip interaction in Eq. (50), which is obtained by treating screening perturbatively through the approximation $\mathcal{W} \approx \mathcal{W}$, takes the form

$$\begin{aligned} \mathcal{V}_{\uparrow\downarrow}^{\cdot\uparrow\downarrow}(12, 34) &= -\delta_{I3}\delta_{24}\mathcal{W}_{\uparrow\uparrow}^{\cdot\uparrow\uparrow}(12) \\ &\quad - \mathcal{P}_{\downarrow\downarrow}^{\cdot\uparrow\downarrow}(13, 24)[\mathcal{W}_{\downarrow\downarrow}^{\cdot\uparrow\downarrow}(13)\mathcal{W}_{\uparrow\downarrow}^{\cdot\uparrow\downarrow}(24) - \cancel{\mathcal{V}_{\downarrow\downarrow}^{\cdot\uparrow\downarrow}(13)\mathcal{V}_{\uparrow\downarrow}^{\cdot\uparrow\downarrow}(24)}] \\ &\quad - \mathcal{P}_{\uparrow\uparrow}^{\cdot\uparrow\downarrow}(13, 24)[\mathcal{W}_{\uparrow\uparrow}^{\cdot\uparrow\downarrow}(13)\mathcal{W}_{\uparrow\uparrow}^{\cdot\uparrow\downarrow}(24) - \cancel{\mathcal{V}_{\uparrow\uparrow}^{\cdot\uparrow\downarrow}(13)\mathcal{V}_{\uparrow\uparrow}^{\cdot\uparrow\downarrow}(24)}] \\ &\quad - \mathcal{P}_{\uparrow\downarrow}^{\cdot\uparrow\downarrow}(13, 24)[\mathcal{W}_{\uparrow\uparrow}^{\cdot\uparrow\downarrow}(14)\mathcal{W}_{\uparrow\downarrow}^{\cdot\uparrow\downarrow}(23) - \mathcal{V}_{\uparrow\uparrow}^{\cdot\uparrow\downarrow}(14)\mathcal{V}_{\uparrow\downarrow}^{\cdot\uparrow\downarrow}(23)] \\ &\quad - \mathcal{P}_{\downarrow\downarrow}^{\cdot\uparrow\downarrow}(13, 24)[\mathcal{W}_{\uparrow\downarrow}^{\cdot\uparrow\downarrow}(14)\mathcal{W}_{\downarrow\downarrow}^{\cdot\uparrow\downarrow}(23) - \mathcal{V}_{\uparrow\downarrow}^{\cdot\uparrow\downarrow}(14)\mathcal{V}_{\downarrow\downarrow}^{\cdot\uparrow\downarrow}(23)] \end{aligned} \quad (55)$$

if ‘‘particle-particle’’ two-point contractions of \mathcal{P} , with $I = 4$ and $2 = 3$, are neglected. The crossed-out spin components of \mathcal{V} in the second and third rows are zero due to crossing symmetry but are kept to illustrate the analogy to the nonvanishing terms in the fourth and fifth rows. The four terms that contain two \mathcal{W} are presented in Fig. 1 and describe the simultaneous propagation of spin and charge excitations. When including lattice vibrations, we will show that they contain the magnon-number-conserving magnon-phonon interaction to second order—the PAMM interaction. If Hedin’s formalism was to be used, the analogous terms to second order in W would miss out on this interaction since W has no spin-flip components. This shows why the PAMM interaction should be expanded in the collective screened four-point interaction \mathcal{W} , which is crossing symmetric, rather than in W . Also the first ‘‘screened T matrix’’ term [77] in Eq. (55) can be generalized to contain phonons, but their effects in this term are averaged out when treating the spin fluctuations as quasiparticles. This will be clarified in the following section.

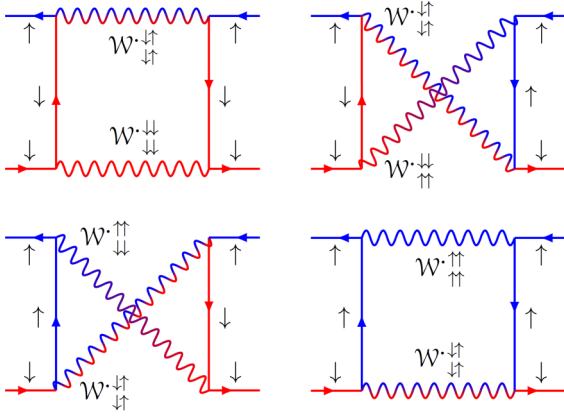


FIG. 1. Diagrammatic representation of the part of the spin-flip interaction describing simultaneous propagation of spin and charge fluctuations. Spin \uparrow and \downarrow Green's functions are distinguished by their colors, and spin conservation in $\mathcal{W}_{\uparrow\downarrow}^{\cdot\downarrow\uparrow}$ is emphasized with the same colors.

C. Two-point approximation in a one-band model

In order to arrive at an efficient approximation with a closer connection to local spin models [48,52,63,78] we contract 1 and 2 as well as 3 and 4 in Eq. (55). It is clear from Fig. 1 that this leaves intact the simultaneous propagation of spin and charge fluctuations. We assume a one-band model and drop the band index since interband couplings are of secondary interest for understanding the effect of phonons. Dropping also the \cdot symbols for convenience, the first term in Eq. (55) is easily made into a one-point quantity through the replacement

$$\mathcal{W}_{\uparrow\downarrow}^{\cdot\downarrow\uparrow}(I2) := \delta_{I2}(\mathcal{U} + \overline{\mathcal{W}}_c), \quad (56)$$

$$\overline{\mathcal{W}}_c = \int_{-\beta/2}^{\beta/2} d\tau \langle \mathcal{W}_{c\uparrow\downarrow}^{\cdot\downarrow\uparrow}(\tau) \rangle_{\text{BZ}}. \quad (57)$$

Here, $\langle \cdots \rangle_{\text{BZ}}$ denotes the Brillouin zone average, and we have used the fact that the two-point \mathcal{W}_c only depends on the relative imaginary time τ . Since the τ dependence is β periodic, the integral is restricted to $[-\beta/2, \beta/2]$ rather than to $[-\beta, \beta]$. The shifted corrections to Eq. (56) are obtained by replacing $\delta_{\tau_1\tau_2}$, implicit in δ_{I2} , with $\delta_{\tau_1, \tau_2 \pm \beta}$. These are excluded since they have no effect on Eq. (46), where all imaginary-time integrals are restricted to the interval $[0, \beta]$. Similarly, the free electron-hole pair propagator, which enters into the remaining terms in Eq. (55), is replaced by the two-point quantity

$$\mathcal{P}_{\sigma\sigma'}^{\sigma\sigma'}(I3, 24) := \delta_{I2}\delta_{34}\overline{\mathcal{G}}_{\sigma}\overline{\mathcal{G}}_{\sigma'}, \quad (58)$$

$$\overline{\mathcal{G}}_{\sigma} = \int_{-\beta/2}^{\beta/2} d\tau \langle \mathcal{G}_{\sigma}(\tau) \rangle_{\text{BZ}}. \quad (59)$$

This integral would vanish if it ranged from $-\beta$ to β due to the antisymmetry of $\overline{\mathcal{G}}_{\sigma}$ under shifts of $-\beta$ in the imaginary-time interval $\tau \in [0, \beta]$. But despite this antisymmetry, the contributions outside the interval $[-\beta/2, \beta/2]$ are suppressed in Eq. (55), motivating the choice of Eq. (59). It is of interest to find an expression for $\overline{\mathcal{G}}_{\sigma}$ since it will be shown to appear in the PAMM interaction when including lattice dynamics. Since we have already broken self-consistency in Sec. III B,

we assume that the Green's function is obtained from a single-particle calculation. In practice this may be a Hartree-Fock or a (spin-)density functional theory [79] calculation. We can then write

$$\langle \mathcal{G}_{\sigma}(\tau) \rangle_{\text{BZ}} = \left\langle \frac{e^{-\xi_{\sigma}\tau}}{e^{\xi_{\sigma}\beta} + 1} \right\rangle_{\text{BZ}} \theta(-\tau) - \left\langle \frac{e^{\xi_{\sigma}(\beta-\tau)}}{e^{\xi_{\sigma}\beta} + 1} \right\rangle_{\text{BZ}} \theta(\tau). \quad (60)$$

ξ_{σ} is shorthand notation for the momentum-dependent spin- σ electronic dispersion $\xi_{\sigma}(\mathbf{k})$ measured relative to the chemical potential μ . The two terms are strongly peaked close to $\tau = 0$ if $\xi_{\sigma}\beta \ll 0$ and $\xi_{\sigma}\beta \gg 0$, respectively, which approximately holds if $\xi_{\sigma} < 0$ and $\xi_{\sigma} > 0$ since typical electronic energy scales are large compared to thermal energies. Consistent with this is the replacement of the exponential functions in the two terms of Eq. (60) with properly normalized δ functions,

$$\langle \mathcal{G}_{\sigma}(\tau) \rangle_{\text{BZ}} \approx \frac{1}{2} \left\langle \frac{\theta(-\xi_{\sigma})}{e^{\xi_{\sigma}\beta} + 1} \int_{-\beta}^0 d\tau' e^{-\xi_{\sigma}\tau'} \right\rangle_{\text{BZ}} \delta(\tau) - \frac{1}{2} \left\langle \frac{e^{\xi_{\sigma}\beta}\theta(\xi_{\sigma})}{e^{\xi_{\sigma}\beta} + 1} \int_0^{\beta} d\tau' e^{-\xi_{\sigma}\tau'} \right\rangle_{\text{BZ}} \delta(\tau), \quad (61)$$

where $\theta(0) = \frac{1}{2}$ has been used twice. By integrating Eq. (61) and using the Fermi occupations $n_{\sigma} = n_F^{\beta}(\xi_{\sigma})$, where $n_F^{\beta}(\omega) = (e^{\omega\beta} + 1)^{-1}$, Eq. (59) becomes

$$\overline{\mathcal{G}}_{\sigma} = \left\langle \frac{n_{\sigma} - 1/2}{|\xi_{\sigma}|} \right\rangle_{\text{BZ}}. \quad (62)$$

This does not, in general, vanish at half filling. The divergence of $1/|\xi_{\sigma}|$ cancels via the numerator. The two-point approximation to the spin-flip interaction in Eq. (55) can now be expressed as

$$\mathcal{V}_{\uparrow\downarrow}^{\uparrow\downarrow}(I2, 34) = -\delta_{I2}\delta_{23}\delta_{34}\mathcal{U} + \delta_{I2}\delta_{34}\Delta_{\uparrow\downarrow}^{\uparrow\downarrow}(I3), \quad (63)$$

where Eqs. (56) and (58) can be used to show that

$$\Delta_{\uparrow\downarrow}^{\uparrow\downarrow}(I2) = -\delta_{I2}\mathcal{U}' - \sum_{\sigma_1\sigma_2} \overline{\mathcal{G}}_{\sigma_1}\overline{\mathcal{G}}_{\sigma_2}\mathcal{W}_{c\uparrow\downarrow}^{\uparrow\downarrow}(I2)\mathcal{W}_{c\sigma_2\sigma_1}^{\sigma_1\sigma_1}(I2), \quad (64)$$

$$\mathcal{U}' = \mathcal{U} \sum_{\sigma_1\sigma_2} \overline{\mathcal{G}}_{\sigma_1}\overline{\mathcal{G}}_{\sigma_2} [\sigma_{\sigma_1\sigma_2}^x \mathcal{W}_{c\uparrow\downarrow}^{\uparrow\downarrow}(I) - \mathcal{W}_{c\sigma_2\sigma_1}^{\sigma_1\sigma_1}(I)] + \overline{\mathcal{W}}_c, \quad (65)$$

where we have abandoned Einstein's summation convention. \mathcal{U}' is a correction to the local interaction, and I in Eq. (65) is short for II . The two-point structure in Eq. (64) allows for an efficient calculation of the spin susceptibility since Eq. (46), which has four-point structure, can be replaced by the two-point equations

$$\mathcal{R}_{\uparrow\downarrow}^{\uparrow\downarrow}(I2) = r_{\uparrow\downarrow}^{\uparrow\downarrow}(I2) + \int d(34)r_{\uparrow\downarrow}^{\uparrow\downarrow}(I3)\Delta_{\uparrow\downarrow}^{\uparrow\downarrow}(34)\mathcal{R}_{\uparrow\downarrow}^{\uparrow\downarrow}(42), \quad (66)$$

$$r_{\uparrow\downarrow}^{\uparrow\downarrow}(I2) = \mathcal{P}_{\uparrow\downarrow}^{\uparrow\downarrow}(I2) - \mathcal{U} \int d3\mathcal{P}_{\uparrow\downarrow}^{\uparrow\downarrow}(I3)r_{\uparrow\downarrow}^{\uparrow\downarrow}(32), \quad (67)$$

where the two-point \mathcal{R} is defined like in Eq. (44) and r is the unperturbed spin susceptibility obtained from only the Fock exchange—the *Fock magnon* propagator. Since Δ is the interaction between Fock magnons in Eq. (66), it can be identified with the magnon-magnon interaction. In momentum and Matsubara space, the *renormalized magnon* propagator of Eq. (66)

reads

$$\mathcal{R}_{\downarrow\uparrow}^{\downarrow\uparrow}(\mathbf{k}, i\omega_m) = \frac{r_{\downarrow\uparrow}^{\downarrow\uparrow}(\mathbf{k}, i\omega_m)}{1 - r_{\downarrow\uparrow}^{\downarrow\uparrow}(\mathbf{k}, i\omega_m)\Delta_{\downarrow\uparrow}^{\downarrow\uparrow}(\mathbf{k}, i\omega_m)}, \quad (68)$$

where $\omega_m = 2\pi m/\beta$. From Eq. (64) it follows that

$$\begin{aligned} \Delta_{\downarrow\uparrow}^{\downarrow\uparrow}(\mathbf{k}, i\omega_m) \\ = -\mathcal{U}' - \frac{1}{N\beta} \sum_{\substack{\mathbf{q}\omega_n \\ \sigma_1\sigma_2}} \bar{\mathcal{G}}_{\sigma_1} \bar{\mathcal{G}}_{\sigma_2} \mathcal{W}_{c\downarrow\uparrow}^{\downarrow\uparrow}(\mathbf{k}-\mathbf{q}, i\omega_m - i\omega_n) \mathcal{W}_{c\sigma_2\sigma_2}^{\sigma_1\sigma_1}(\mathbf{q}, i\omega_n), \end{aligned} \quad (69)$$

where N is the number of \mathbf{k} points in the Brillouin zone.

D. Phonon-assisted magnon-magnon interaction

We now deform the $\mathcal{W}_{c\sigma_2\sigma_2}^{\sigma_1\sigma_1}$ component of \mathcal{W}_c in Eq. (69) to include phonons, as anticipated throughout this paper. Following the works of Hedin and Lundqvist [71] and Giustino [70], where the nuclear spin is neglected, it can be split into a term of electronic charge fluctuations (plasmons) and one which contains the phonons. Assuming a single phonon mode $\nu = P$ (P for phonon), we get

$$\mathcal{W}_{c\sigma_2\sigma_2}^{\sigma_1\sigma_1}(\mathbf{q}, i\omega_n) := \mathcal{W}_{c\sigma_2\sigma_2}^{\sigma_1\sigma_1}(\mathbf{q}, i\omega_n) + g_{\mathbf{q}}^{\sigma_1} g_{\mathbf{q}}^{\sigma_2*} \mathcal{D}(\mathbf{q}, i\omega_n), \quad (70)$$

where

$$g_{\mathbf{q}}^{\sigma} = \frac{1}{N} \sum_k g_{mn, \nu=P}^{\sigma}(\mathbf{k}, \mathbf{q}) \quad (71)$$

is the one-momentum electron-phonon interaction between the electrons in the band of our one-band model n (which we drop) and the phonons in branch $\nu = P$ and

$$\mathcal{D}(\mathbf{q}, i\omega_n) = \frac{2\omega_{\mathbf{q}}^P}{(i\omega_n)^2 - (\omega_{\mathbf{q}}^P)^2} \quad (72)$$

is the phonon propagator in the adiabatic approximation, determined from the phonon dispersion $\omega_{\mathbf{q}}^P \geq 0$, neglecting lifetime broadening. Nothing in our formalism requires this simplification, but it allows for analytic Matsubara summation. Extending to several electron bands and phonon modes is straightforward, but the momentum average and band diagonality in Eq. (71) follow from the two-point contraction in Sec. III C. From Ref. [70], we find

$$g_{\mathbf{q}}^{\sigma} = \frac{-Z}{\sqrt{2M\omega_{\mathbf{q}}^P}} (\mathbf{e}_{\mathbf{q}}^P \cdot \mathcal{F}_{\mathbf{q}}^{\sigma}) \quad (73)$$

if we assume a single (light) atom in each unit cell, with atomic number Z , mass M , and equilibrium position $\boldsymbol{\tau}^{(0)}$ in the central cell. $\mathbf{e}_{\mathbf{q}}^P$ is the phonon polarization, and

$$\mathcal{F}_{\mathbf{q}}^{\sigma} = \sum_{\mathbf{T}} e^{i\mathbf{q}\cdot\mathbf{T}} \int d\mathbf{r} w_{\mathbf{0}}^*(\mathbf{r}) \mathcal{F}_{\sigma}(\mathbf{r}, \mathbf{T}) w_{\mathbf{0}}(\mathbf{r}) \quad (74)$$

are Fourier components of the diagonal Wannier matrix elements in the central unit cell of the ‘‘screened force’’ from the nuclei (or ions) in the \mathbf{T} -shifted unit cells,

$$\mathcal{F}_{\sigma}(\mathbf{r}, \mathbf{T}) = \sum_{\sigma'} \int d\mathbf{r}' [\mathcal{S}^{-1}]_{\sigma'\sigma}^{\sigma\sigma}(\mathbf{r}\mathbf{r}') \frac{(\mathbf{r}' - \mathbf{T} - \boldsymbol{\tau}^{(0)})}{|\mathbf{r}' - \mathbf{T} - \boldsymbol{\tau}^{(0)}|^3}. \quad (75)$$

\mathcal{S}^{-1} is here the spin-dependent finite-temperature analog of the static ϵ^{-1} in Ref. [70]. Equation (70) and ($\bar{\sigma} = -\sigma$)

$$\mathcal{W}_{c\downarrow\uparrow}^{\downarrow\uparrow}(\mathbf{q}, i\omega_n) = \mathcal{U}^2 r_{\downarrow\uparrow}^{\downarrow\uparrow}(\mathbf{q}, i\omega_n), \quad (76)$$

$$\mathcal{W}_{c\sigma_2\sigma_2}^{\sigma_1\sigma_1}(\mathbf{q}, i\omega_n) = \mathcal{U}^2 r_{\bar{\sigma}_2\bar{\sigma}_2}^{\bar{\sigma}_1\bar{\sigma}_1}(\mathbf{q}, i\omega_n), \quad (77)$$

which hold since $\mathcal{W}_c = \mathcal{W}_{c\bar{\cdot}}$, turn Eq. (69) into

$$\begin{aligned} \Delta_{\downarrow\uparrow}^{\downarrow\uparrow}(\mathbf{k}, i\omega_m) = -\mathcal{U}'_{\mathcal{D}} - \frac{\mathcal{U}^2}{N\beta} \sum_{\substack{\mathbf{q}\omega_n \\ \sigma_1\sigma_2}} \bar{\mathcal{G}}_{\sigma_1} \bar{\mathcal{G}}_{\sigma_2} r_{\downarrow\uparrow}^{\downarrow\uparrow}(\mathbf{k}-\mathbf{q}, i\omega_m - i\omega_n) \\ \times [\mathcal{U}^2 r_{\bar{\sigma}_2\bar{\sigma}_2}^{\bar{\sigma}_1\bar{\sigma}_1}(\mathbf{q}, i\omega_n) + g_{\mathbf{q}}^{\sigma_1} \mathcal{D}(\mathbf{q}, i\omega_n) g_{\mathbf{q}}^{\sigma_2*}], \end{aligned} \quad (78)$$

where $\mathcal{U}'_{\mathcal{D}}$ is the modified \mathcal{U}' due to the phonons. The first term of the magnon-magnon interaction in Eq. (78) is quadratic in the magnon-number-conserving interaction between Fock magnons and longitudinal spin fluctuations as well as electronic charge fluctuations (plasmons), and the second term is quadratic in the magnon-number-conserving magnon-phonon interaction—it is the sought-after PAMM interaction Δ_{PA} . Since, typically, only the magnon and phonon energies are comparable, we keep only the last term in the following. Furthermore, the term $\mathcal{U}'_{\mathcal{D}}$ will be considered fixed by the Goldstone criterion, which requires that the magnon dispersion contained in the imaginary part of $\mathcal{R}_{\downarrow\uparrow}^{\downarrow\uparrow}$ in Eq. (68) approach zero in the long-wavelength limit, $\mathbf{k} \rightarrow \mathbf{0}$. It remains to find $r_{\downarrow\uparrow}^{\downarrow\uparrow}$, but since it is generated by the local and instantaneous interaction \mathcal{U} , it lacks lifetime broadening and is accurately parametrized as

$$r_{\downarrow\uparrow}^{\downarrow\uparrow}(\mathbf{k}, i\omega_m) = \frac{1}{i\omega_m - \omega_{\mathbf{k}}^M} \quad (79)$$

in terms of the Fock magnon dispersion $\omega_{\mathbf{k}}^M \geq 0$, treated as temperature independent for simplicity. The positivity holds since \uparrow is the majority spin channel. In practice, Eq. (79) can be matched to first-principles calculations of $r_{\downarrow\uparrow}^{\downarrow\uparrow}$ based on Eq. (67). The PAMM interaction term in Eq. (78) can be written in a physically transparent form by making use of Eqs. (72) and (79) and performing Matsubara summation and analytic continuation ($i\omega_m \rightarrow \omega + i\eta$). The result is

$$\begin{aligned} \Delta_{\text{PA}\downarrow\uparrow}^{\downarrow\uparrow}(\mathbf{k}, \omega) \\ = \mathcal{U}^2 \int \frac{d\mathbf{q}}{\Omega_{\text{BZ}}} |\bar{\mathcal{G}}_{\uparrow} g_{\mathbf{q}}^{\uparrow} + \bar{\mathcal{G}}_{\downarrow} g_{\mathbf{q}}^{\downarrow}|^2 \\ \times \left(\frac{n_{\mathbf{q}}^P - n_{\mathbf{k}-\mathbf{q}}^M}{\omega + \omega_{\mathbf{q}}^P - \omega_{\mathbf{k}-\mathbf{q}}^M + i\eta} + \frac{1 + n_{\mathbf{q}}^P + n_{\mathbf{k}-\mathbf{q}}^M}{\omega - \omega_{\mathbf{q}}^P - \omega_{\mathbf{k}-\mathbf{q}}^M + i\eta} \right), \end{aligned} \quad (80)$$

where $n_{\mathbf{q}}^{M/P} = n_B^{\beta}(\omega_{\mathbf{q}}^{M/P})$ and $n_B^{\beta}(\omega) = (e^{\beta\omega} - 1)^{-1}$ is the magnon/phonon Bose occupation. The superscript r emphasizes that it is the retarded interaction. Likewise, the retarded Fock magnon propagator $r_{\downarrow\uparrow}^{r\downarrow\uparrow}$ and renormalized magnon propagator $\mathcal{R}_{\downarrow\uparrow}^{r\downarrow\uparrow}$ are obtained by analytically continuing Eqs. (79) and (68), respectively, where the latter is determined from the former and the retarded PAMM interaction in Eq. (80), up to the Goldstone shift. In Eq. (80), the continuous limit $\frac{1}{N} \sum_{\mathbf{k}} \rightarrow \int \frac{d\mathbf{q}}{\Omega_{\text{BZ}}}$ has been taken, where Ω_{BZ} is the Brillouin zone volume. The two terms describe phonon absorption and

emission, respectively, and only the emission term survives in the limit $T \rightarrow 0$. Except for the fact that Eq. (80) is not restricted to acoustic phonons, it has the same form as the nonrelativistic contribution to Eq. (4.4) in Ref. [63], where the interaction was derived using a phenomenological magnetoelastic model. This suggests that the present work provides a path beyond such models by avoiding one or several of the assumptions made to arrive at Eq. (80). The inclusion of spin-orbit interaction and, consequently, anisotropy will be discussed in a future paper.

IV. MODEL CALCULATIONS

A. Introducing the model

A minimal three-dimensional model is considered in which the retarded PAMM interaction in Eq. (80) is momentum independent while retaining energy dependence. To this aim, we assume an isotropic magnon dispersion ω_q^m , where $q = |q|$, and a dispersionless optical phonon ω^p ; replace the spin-dependent electron-phonon interaction g_q^σ with its spin average g_q ; replace $|g_q|^2$ with its Brillouin zone average \bar{g}^2 [80]; and, finally, approximate the Brillouin zone integral of any isotropic function with an integral over a sphere with matching volume, i.e., with radius $K = (3\Omega_{\text{BZ}}/4\pi)^{1/3}$. Equation (80) then takes the simple form

$$\begin{aligned} \Delta_{\text{PA}\uparrow\downarrow}^r(\omega) &= \mathcal{A}^2 \int_0^K \frac{4\pi q^2 dq}{\Omega_{\text{BZ}}} \\ &\times \left(\frac{n^p - n_q^m}{\omega + \omega^p - \omega_q^m + i\eta} + \frac{1 + n^p + n_q^m}{\omega - \omega^p - \omega_q^m + i\eta} \right), \end{aligned} \quad (81)$$

where we have introduced the (positive) magnon-phonon interaction strength

$$\mathcal{A} = u|\bar{g}_\uparrow + \bar{g}_\downarrow| \sqrt{\bar{g}^2}. \quad (82)$$

This has the dimension of energy, for which we, in the following, will use units of eV rather than Hartrees. In the results that follow, we tune \mathcal{A} independently of temperature. We also use a typical optical phonon energy of $\omega^p = 0.05$ eV, chosen to be in the middle of the isotropic magnon band, which we parametrize as $\omega_q^m = 0.1 \sin^2(\frac{q\pi}{2K})$ eV, with the typical value $K = \pi/a$, with $a = 7$ in atomic units, assumed to be temperature independent. The retarded PAMM interaction in Eq. (81) will be complemented by a shift to guarantee that the Goldstone criterion is satisfied.

B. Results

The real and imaginary parts of the retarded PAMM interaction Δ_{PA}^r in Eq. (81) are presented in Fig. 2 at temperatures of 0 and 300 K (room temperature) for an interaction strength of $\mathcal{A} = 32$ meV. The convergence parameter η is chosen to be 0.3 meV. The results for different values of \mathcal{A} are the same up to the overall scaling. The main dispersion feature present both at absolute zero and at room temperature describes phonon emission and occurs around 0.15 eV. This therefore originates partly from the ‘‘zero-temperature term’’

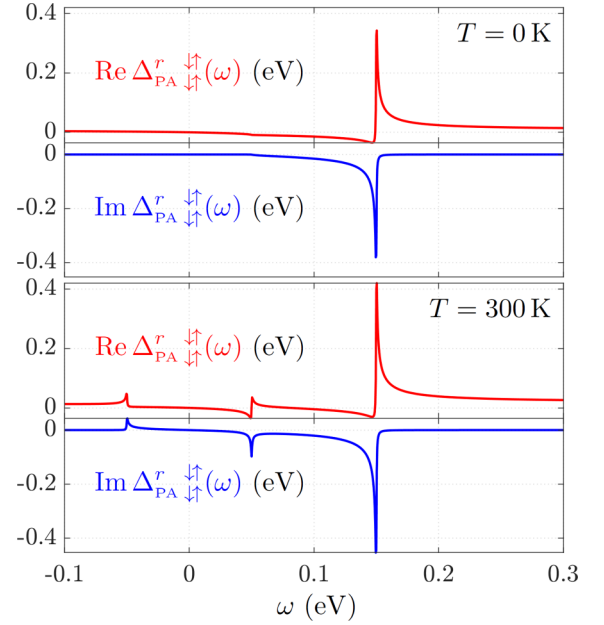


FIG. 2. Real and imaginary parts of the PAMM interaction $\Delta_{\text{PA}\uparrow\downarrow}^r(\omega)$ at $T = 0$ K and $T = 300$ K, with $\mathcal{A} = 32$ meV.

in Eq. (81) that lacks both phonon and Fock magnon (FM) Bose occupation factors. The energy is understood by adding a phonon energy of 0.05 to 0.1 eV, for which the FM spectral density is the largest. Temperature enhances this feature but also induces dispersion features corresponding to phonon absorption at energies ± 0.05 eV, caused by the first term in Eq. (81). This gets large either for FM energies close to zero, where the Bose occupation is large, or for FM energies close to 0.01 eV, with large spectral weight, explaining the two features. In our particular model, the phonon energy of 0.05 eV coincides with the difference between the predominant energy of 0.1 eV of the FM and that of the phonons.

The magnitude of the renormalized magnon (RM) spectral function, $A^M(k, \omega) = -\frac{1}{\pi} \text{Im} \mathcal{R}^{\uparrow\downarrow}(k, \omega)$, is shown in Fig. 3 for different values of \mathcal{A} at $T = 0$ K and $T = 300$ K. With increased \mathcal{A} , the zero-temperature RM spectrum acquires an increasingly significant background continuum in the range between 0.05 and 0.15 eV, where the imaginary part of Δ_{PA}^r dominates, as well as a sharp spectral peak above this range in the form of a satellite feature, where the real part dominates (see Fig. 2). This feature can be understood by combining the analytically continued Eqs. (68) and (79), which in our model and the limit $\eta \rightarrow 0$ imply that

$$A^M(k, \omega) = \frac{-\frac{1}{\pi} \text{Im} \Delta_{\text{PA}\uparrow\downarrow}^r(\omega)}{[\omega - \omega_k^m - \text{Re} \Delta_{\text{PA}\uparrow\downarrow}^r(\omega)]^2 + [\text{Im} \Delta_{\text{PA}\uparrow\downarrow}^r(\omega)]^2}. \quad (83)$$

A quasiparticle peak is expected if $\omega - \omega_k^m = \text{Re} \Delta_{\text{PA}\uparrow\downarrow}^r(\omega)$, which can be solved graphically in Fig. 2 for the case $\mathcal{A} = 32$ meV. For example, at $k = K$ we can plug in $\omega_k^m = 0.1$ eV and find three intersection energies, ω_1 , ω_2 , and ω_3 . In the zero-temperature case, as a consequence of the phonon emission feature in $\text{Re} \Delta_{\text{PA}\uparrow\downarrow}^r(\omega)$, ω_1 is slightly reduced compared to the original magnon energy 0.1 eV, whereas $\omega_2 \approx 0.15$ eV

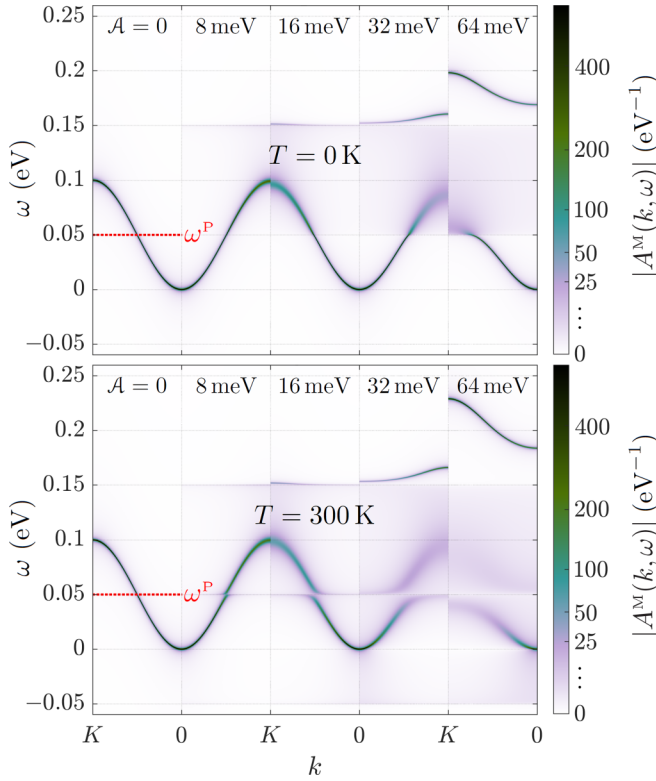


FIG. 3. Magnitude of the renormalized magnon spectral function $A^M(k, \omega)$ at $T = 0$ K and $T = 300$ K for various \mathcal{A} .

and $\omega_3 \approx 0.16$ eV are increased. For each of these intersection energies, it holds that

$$A^M(K, \omega_i) = -\frac{1}{\pi} \frac{1}{\text{Im} \Delta_{\text{PA}\downarrow\uparrow}^r(\omega_i)}, \quad i = 1, 2, 3. \quad (84)$$

This means that the relative weights of the three expected peaks are dictated by the inverse of $\text{Im} \Delta_{\text{PA}\downarrow\uparrow}^r(\omega_i)$, which is also deducible from Fig. 2. There, we see that the imaginary part is weakly negative at ω_1 and ω_3 but strongly negative at ω_2 . This explains why we, in the zero-temperature plot at $\mathcal{A} = 32$ meV in Fig. 3, see only two peaks in A^M at $k = K$, one slightly below 0.1 eV and one around 0.16 eV. Indeed, the suppression of a peak at ω_2 is a consequence of the fact that the corresponding intersection point in Fig. 2 is unphysical since $\text{Re} \Delta_{\text{PA}\downarrow\uparrow}^r(\omega)$ in the limit $\eta \rightarrow 0$ would jump immediately from $-\infty$ up to ∞ at 0.15 eV.

At room temperature, we see from Fig. 3 that the background continuum in A^M stretches from -0.05 to 0.15 eV and that the satellite feature associated with phonon emission gets accompanied by a splitting of the RM band associated with phonon absorption around 0.05 eV—the energy difference between the FM band maximum and the phonon. Like the sharp satellite feature, the splitting occurring at $k = K/2$ can also be understood by the method of intersections used above. However, since $\text{Im} \Delta_{\text{PA}\downarrow\uparrow}^r(\omega)$ does not decay rapidly either below or above 0.05 eV, no sharp quasiparticle splitting is generally observed. For this same reason, the broad Hubbard-like splitting, which notably is observed also at $k = K$ when $\mathcal{A} = 32$ meV, cannot be deduced by the method of intersections since it does not correspond to any quasiparticle solutions.

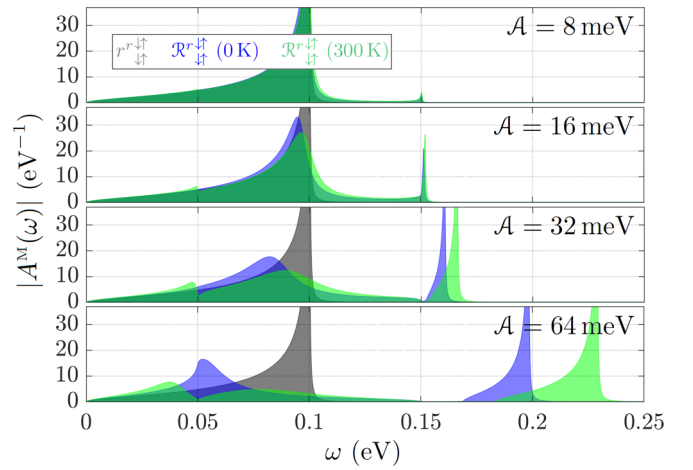


FIG. 4. Magnitude of the total spectral function $A^M(\omega)$ for Fock magnons $r_{\downarrow\uparrow}^r$ and renormalized magnons $\mathcal{R}_{\downarrow\uparrow}^r$ at $T = 0$ K and $T = 300$ K for various \mathcal{A} .

The magnitude of the total RM spectral function, $A^M(\omega) = \int_0^K \frac{4\pi k^2 dk}{\Omega_{\text{BZ}}} A^M(k, \omega)$, is presented in Fig. 4 for different \mathcal{A} at absolute zero and room temperature and is compared with the results of the FM. The temperature-induced splitting at 0.05 eV is shown to increase the low-energy spectral weight. The product of the Bose occupation and the total spectrum $n_B^\beta(\omega)A^M(\omega)$, which is strictly positive and proportional to the temperature-dependent probability of finding a magnon with energy ω , is presented in Fig. 5 at different temperatures for the FM and the RM, using $\mathcal{A} = 64$ meV. Since each

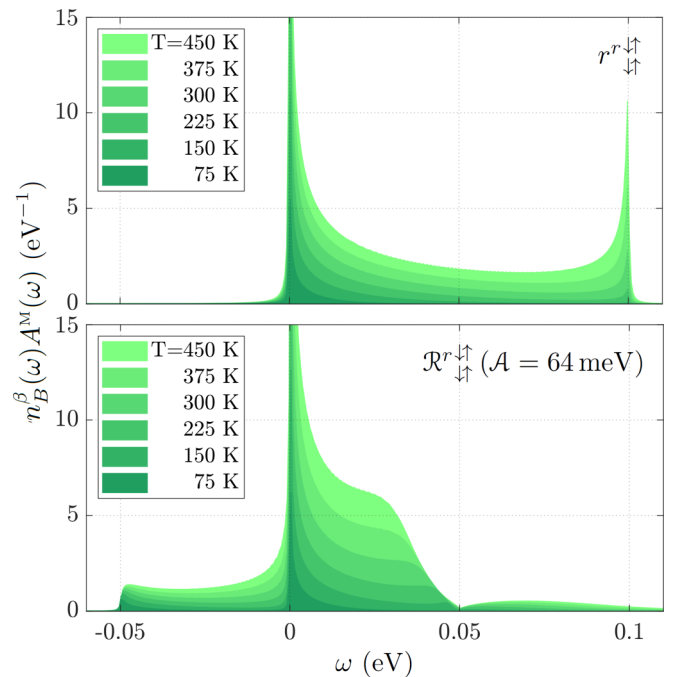


FIG. 5. Product of Bose occupation $n_B^\beta(\omega)$ and magnon spectrum $A^M(\omega)$ for Fock magnons $r_{\downarrow\uparrow}^r$ and renormalized magnons $\mathcal{R}_{\downarrow\uparrow}^r$ at various temperatures. $\mathcal{A} = 64$ meV.

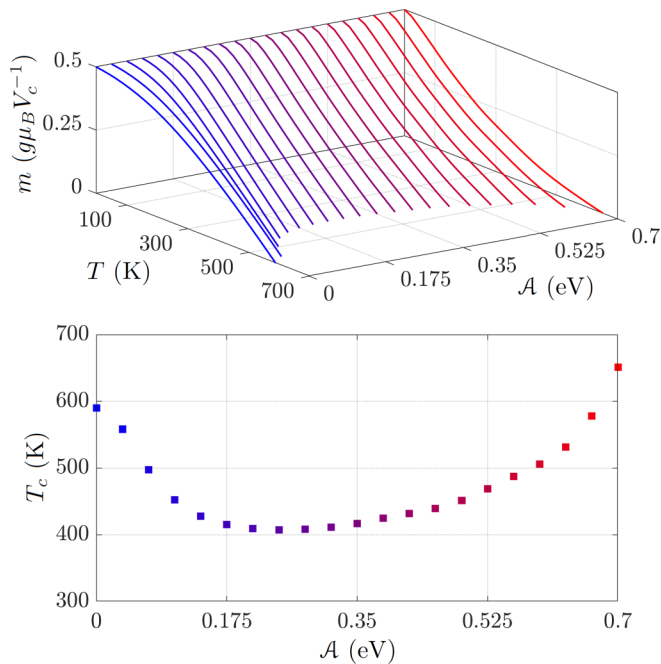


FIG. 6. Spin magnetization m as a function of T for different values of \mathcal{A} , together with the associated Curie temperatures T_c for which $m = 0$.

magnon carries an angular momentum of 1, the energy integral of this product precisely yields the temperature-induced reduction of the spin magnetization after we divide by the unit cell volume V_c and $g\mu_B = 1$, where $g = 2$ is the g factor and $\mu_B = \frac{1}{2}$ is the Bohr magneton. Assuming that the spin magnetization per unit volume at $T = 0$ is $0.5g\mu_B$, the temperature-dependent magnetization is shown in Fig. 6 for different \mathcal{A} . The \mathcal{A} -dependent Curie temperature at which the magnetization vanishes is also presented. For $\mathcal{A} = 0$ and low temperatures the thermally accessible magnons can be approximated as parabolic so that the famous $T^{3/2}$ law for the magnetization is reproduced. When increasing \mathcal{A} from zero, the Curie temperature decreases due to an increase in the low-energy RM spectral weight, originating from the band narrowing below 0.05 eV due to the splitting. However, when continuing to increase \mathcal{A} the Curie temperature starts to in-

crease again as a consequence of a washing out of the RM spectral weight.

V. SUMMARY AND OUTLOOK

In this work, we have provided a formalism for phonon-assisted magnon-magnon interaction, which is quadratic in the magnon-number-conserving magnon-phonon interaction. By assuming quenched orbital magnetic moments and neglecting spin-orbit interaction, the poorly understood exchange-mediated contribution was isolated.

By writing the electron-electron interaction in a crossing-symmetric way and using Schwinger's functional derivative method, we identified the *screened collective* four-point interaction \mathcal{W} as the natural many-body expansion parameter. After resorting to a Hubbard-like model, we showed by iteration after a two-point contraction how the magnon-magnon interaction acquires terms quadratic in \mathcal{W} that describe simultaneous propagation of spin and charge fluctuations. By relaxing the clamped-nuclei approximation, we arrived at a phonon-assisted magnon-magnon interaction [Eq. (80)] of the same form as derived from phenomenological magnetoelastic models but with first-principles access to the magnon-phonon coupling strength from the underlying electronic structure. We tested the formula on a model with isotropic magnons and dispersion-free phonons and found a temperature-induced low-energy magnon splitting due to phonon absorption which reduced the Curie temperature.

The developed formalism will be extended to account for spin-orbit interaction and other semirelativistic effects in a future publication. Another line of inquiry is to investigate how the PAMM interaction of Eq. (80) affects the *ab initio* critical temperature in high-temperature superconductors by studying the gap equation. The PAMM interaction can also be readily extended to nonequilibrium to study magnetoelastic effects on magnonics in the presence of thermal gradients.

ACKNOWLEDGMENTS

We acknowledge valuable discussions with S. Biermann and financial support from the Swedish Research Council (Vetenskapsrådet, VR) and the Knut and Alice Wallenberg (KAW) Foundation.

-
- [1] B. Liao, A. A. Maznev, K. A. Nelson, and G. Chen, *Nat. Commun.* **7**, 13174 (2016).
 - [2] M. Eichenfield, J. Chan, R. M. Camacho, K. J. Vahala, and O. Painter, *Nature (London)* **462**, 78 (2009).
 - [3] M. Aspelmeyer, T. J. Kippenberg, and F. Marquardt, *Rev. Mod. Phys.* **86**, 1391 (2014).
 - [4] A. A. Serga, A. V. Chumak, and B. Hillebrands, *J. Phys. D* **43**, 264002 (2010).
 - [5] L. J. Cornelissen, J. Liu, R. A. Duine, J. Ben Youssef, and B. J. van Wees, *Nat. Phys.* **11**, 1022 (2015).
 - [6] A. V. Chumak, V. I. Vasyuchka, A. A. Serga, and B. Hillebrands, *Nat. Phys.* **11**, 453 (2015).
 - [7] S. O. Demokritov, V. E. Demidov, O. Dzyapko, G. A. Melkov, A. A. Serga, B. Hillebrands, and A. N. Slavin, *Nature (London)* **443**, 430 (2006).
 - [8] A. Rückriegel and P. Kopietz, *Phys. Rev. Lett.* **115**, 157203 (2015).
 - [9] D. J. Scalapino, *Rev. Mod. Phys.* **84**, 1383 (2012).
 - [10] F. Essenberg, A. Sanna, A. Linscheid, F. Tandetzky, G. Profeta, P. Cudazzo, and E. K. U. Gross, *Phys. Rev. B* **90**, 214504 (2014).
 - [11] P. Dai, H. Y. Hwang, J. Zhang, J. A. Fernandez-Baca, S.-W. Cheong, C. Kloc, Y. Tomioka, and Y. Tokura, *Phys. Rev. B* **61**, 9553 (2000).

- [12] C. Berk, M. Jaris, W. Yang, S. Dhuey, S. Cabrini, and H. Schmidt, *Nat. Commun.* **10**, 2652 (2019).
- [13] C. R. Berk and H. Schmidt, *Physics* **13**, 167 (2020).
- [14] H. Man, Z. Shi, G. Xu, Y. Xu, X. Chen, S. Sullivan, J. Zhou, K. Xia, J. Shi, and P. Dai, *Phys. Rev. B* **96**, 100406(R) (2017).
- [15] B. Ramachandran, K. K. Wu, Y. K. Kuo, and M. S. Ramachandra Rao, *J. Phys. D* **48**, 115301 (2015).
- [16] R. Valdés Aguilar, A. B. Sushkov, C. L. Zhang, Y. J. Choi, S.-W. Cheong, and H. D. Drew, *Phys. Rev. B* **76**, 060404(R) (2007).
- [17] F. Körmann, B. Grabowski, B. Dutta, T. Hickel, L. Mauger, B. Fultz, and J. Neugebauer, *Phys. Rev. Lett.* **113**, 165503 (2014).
- [18] D. Perera, D. M. Nicholson, M. Eisenbach, G. M. Stocks, and D. P. Landau, *Phys. Rev. B* **95**, 014431 (2017).
- [19] C. M. Jaworski, J. Yang, S. Mack, D. D. Awschalom, R. C. Myers, and J. P. Heremans, *Phys. Rev. Lett.* **106**, 186601 (2011).
- [20] T. Kikkawa, K. Shen, B. Flebus, R. A. Duine, K. I. Uchida, Z. Qiu, G. E. W. Bauer, and E. Saitoh, *Phys. Rev. Lett.* **117**, 207203 (2016).
- [21] B. Flebus, K. Shen, T. Kikkawa, K. I. Uchida, Z. Qiu, E. Saitoh, R. A. Duine, and G. E. W. Bauer, *Phys. Rev. B* **95**, 144420 (2017).
- [22] R. Yahiro, T. Kikkawa, R. Ramos, K. Oyanagi, T. Hioki, S. Daimon, and E. Saitoh, *Phys. Rev. B* **101**, 024407 (2020).
- [23] K. Uchida, H. Adachi, T. An, T. Ota, M. Toda, B. Hillebrands, S. Maekawa, and E. Saitoh, *Nat. Mater.* **10**, 737 (2011).
- [24] G. E. W. Bauer, E. Saitoh, and B. J. van Wees, *Nat. Mater.* **11**, 391 (2012).
- [25] M. Weiler, H. Huebl, F. S. Goerg, F. D. Czeschka, R. Gross, and S. T. B. Goennenwein, *Phys. Rev. Lett.* **108**, 176601 (2012).
- [26] H. Hayashi and K. Ando, *Phys. Rev. Lett.* **121**, 237202 (2018).
- [27] P. A. Sharma, J. S. Ahn, N. Hur, S. Park, S. B. Kim, S. Lee, J.-G. Park, S. Guha, and S.-W. Cheong, *Phys. Rev. Lett.* **93**, 177202 (2004).
- [28] H. Katsura, N. Nagaosa, and P. A. Lee, *Phys. Rev. Lett.* **104**, 066403 (2010).
- [29] L. Zhang and Q. Niu, *Phys. Rev. Lett.* **112**, 085503 (2014).
- [30] D. A. Garanin and E. M. Chudnovsky, *Phys. Rev. B* **92**, 024421 (2015).
- [31] J. Holanda, D. S. Maior, A. Azevedo, and S. M. Rezende, *Nat. Phys.* **14**, 500 (2018).
- [32] N. Ogawa, W. Koshibae, A. J. Beekman, N. Nagaosa, M. Kubota, M. Kawasaki, and Y. Tokura, *Proc. Natl. Acad. Sci. U.S.A.* **112**, 8977 (2015).
- [33] X. Zhang, Y. Zhang, S. Okamoto, and D. Xiao, *Phys. Rev. Lett.* **123**, 167202 (2019).
- [34] K. An, K. S. Olsson, A. Weathers, S. Sullivan, X. Chen, X. Li, L. G. Marshall, X. Ma, N. Klimovich, J. Zhou, L. Shi, and X. Li, *Phys. Rev. Lett.* **117**, 107202 (2016).
- [35] V. V. Struzhkin, *Low Temp. Phys.* **42**, 884 (2016).
- [36] D. A. Bozhko, P. Clausen, G. A. Melkov, V. S. L'vov, A. Pomyalov, V. I. Vasyuchka, A. V. Chumak, B. Hillebrands, and A. A. Serga, *Phys. Rev. Lett.* **118**, 237201 (2017).
- [37] L. D. Landau and E. M. Lifshitz, *Phys. Z. Sowjetunion* **8**, 153 (1935).
- [38] E. Abrahams and C. Kittel, *Phys. Rev.* **88**, 1200 (1952).
- [39] C. Kittel and E. Abrahams, *Rev. Mod. Phys.* **25**, 233 (1953).
- [40] C. Kittel, *Phys. Rev.* **110**, 836 (1958).
- [41] M. I. Kaganov and V. M. Tsukernik, *Sov. Phys. JETP* **9**, 151 (1959).
- [42] H. F. Tiersten, *J. Math. Phys.* **5**, 1298 (1964).
- [43] E. Schlömann and R. Joseph, *J. Appl. Phys.* **35**, 2382 (1964).
- [44] E. Pytte, *Ann. Phys. (NY)* **32**, 377 (1965).
- [45] R. Silbergliitt, *Phys. Rev.* **188**, 786 (1969).
- [46] S. M. Rezende and F. R. Morgenthaler, *J. Appl. Phys.* **40**, 524 (1969).
- [47] S. C. Guerreiro and S. M. Rezende, *Rev. Bras. Fis.* **1**, 207 (1971).
- [48] J. Jensen and J. G. Houmann, *Phys. Rev. B* **12**, 320 (1975).
- [49] E. N. Economou, K. L. Ngai, T. L. Reinecke, J. Ruvalds, and Richard Silbergliitt, *Phys. Rev. B* **13**, 3135 (1976).
- [50] D. U. Sanger, *Phys. Rev. B* **49**, 12176 (1994).
- [51] L. M. Woods, *Phys. Rev. B* **65**, 014409 (2001).
- [52] T.-M. Cheng and L. Li, *J. Magn. Magn. Mater.* **320**, 1 (2008).
- [53] M. Berciu and G. A. Sawatzky, *Phys. Rev. B* **79**, 195116 (2009).
- [54] A. Ruckriegel, P. Kopietz, D. A. Bozhko, A. A. Serga, and B. Hillebrands, *Phys. Rev. B* **89**, 184413 (2014).
- [55] S. C. Guerreiro and S. M. Rezende, *Phys. Rev. B* **92**, 214437 (2015).
- [56] A. Kamra, H. Keshtgar, P. Yan, and G. E. W. Bauer, *Phys. Rev. B* **91**, 104409 (2015).
- [57] A. L. Chernyshev and W. Brenig, *Phys. Rev. B* **92**, 054409 (2015).
- [58] R. Takahashi and N. Nagaosa, *Phys. Rev. Lett.* **117**, 217205 (2016).
- [59] S. F. Maehrlein, I. Radu, P. Maldonado, A. Paarmann, M. Gensch, A. M. Kalashnikova, R. V. Pisarev, M. Wolf, P. M. Oppeneer, J. Barker, and T. Kampfrath, *Sci. Adv.* **4**, eaar5164 (2018).
- [60] R. Schmidt, F. Wilken, T. S. Nunner, and P. W. Brouwer, *Phys. Rev. B* **98**, 134421 (2018).
- [61] S. L. Holm, A. Kreisel, T. K. Schaffer, A. Bakke, M. Bertelsen, U. B. Hansen, M. Retuerto, J. Larsen, D. Prabhakaran, P. P. Deen, Z. Yamani, J. O. Birk, U. Stuhr, Ch. Niedermayer, A. L. Fennell, B. M. Andersen, and K. Lefmann, *Phys. Rev. B* **97**, 134304 (2018).
- [62] B. Zare Rameshti and R. A. Duine, *Phys. Rev. B* **99**, 060402(R) (2019).
- [63] S. Streib, N. Vidal-Silva, K. Shen, and G. E. W. Bauer, *Phys. Rev. B* **99**, 184442 (2019).
- [64] L. Chotorlishvili, X.-G. Wang, Z. Toklikishvili, and J. Berakdar, *Phys. Rev. B* **97**, 144409 (2018).
- [65] S. M. Rezende, D. S. Maior, O. Alves Santos, and J. Holanda, *Phys. Rev. B* **103**, 144430 (2021).
- [66] V. P. Antropov, M. I. Katsnelson, B. N. Harmon, M. van Schilfgaarde, and D. Kusnezov, *Phys. Rev. B* **54**, 1019 (1996).
- [67] M.-C. Ciornei, J. M. Rubı, and J.-E. Wegrowe, *Phys. Rev. B* **83**, 020410(R) (2011).
- [68] S. Bhattacharjee, L. Nordstrom, and J. Fransson, *Phys. Rev. Lett.* **108**, 057204 (2012).
- [69] J. Fransson, D. Thonig, P. F. Bessarab, S. Bhattacharjee, J. Hellsvik, and L. Nordstrom, *Phys. Rev. Materials* **1**, 074404 (2017).
- [70] F. Giustino, *Rev. Mod. Phys.* **89**, 015003 (2017).
- [71] L. Hedin and S. Lundqvist, *Solid State Phys.* **23**, 1 (1970).
- [72] T. Ayral, J. Vucicevic, and O. Parcollet, *Phys. Rev. Lett.* **119**, 166401 (2017).

- [73] L. Hedin, *Phys. Rev.* **139**, A796 (1965).
- [74] R. Starke and G. A. H. Schober, *Photonics Nanostruct. Fund. Appl.* **14**, 1 (2015).
- [75] G. Onida, L. Reining, and A. Rubio, *Rev. Mod. Phys.* **74**, 601 (2002).
- [76] A. L. Kutepov and G. Kotliar, *Phys. Rev. B* **96**, 035108 (2017).
- [77] E. Sasioglu, A. Schindlmayr, C. Friedrich, F. Freimuth, and S. Blügel, *Phys. Rev. B* **81**, 054434 (2010).
- [78] J. Hellsvik, D. Thonig, K. Modin, D. Iuşan, A. Bergman, O. Eriksson, L. Bergqvist, and A. Delin, *Phys. Rev. B* **99**, 104302 (2019).
- [79] C. R. Jacob and M. Reiher, *Int. J. Quantum Chem.* **112**, 3661 (2012).
- [80] G. L. Goodvin and M. Berciu, *Phys. Rev. B* **78**, 235120 (2008).

Correction: The copyright license statement was presented incorrectly and has been fixed.